

Research on Stability of MMC-Based Medium Voltage DC Bus on Ships Based on Lyapunov Method

Liang FANG^{†a)}, Xiaoyan XU[†], and Tomasz TARASIUK^{††}, *Nonmembers*

SUMMARY Modular multilevel converters (MMCs) are an emerging and promising option for medium voltage direct current (MVDC) of all-electric ships. In order to improve the stability of the MVDC transmission system for ships, this paper presents a new control inputs-based Lyapunov strategy based on feedback linearization. Firstly, a set of dynamics equations is proposed based on separating the dynamics of AC-part currents and MMCs circulating currents. The new control inputs can be obtained by the use of feedback linearization theory applied to the dynamic equations. To complete the dynamic parts of the new control inputs from the viewpoint of MVDC system stability, the Lyapunov theory is designed some compensators to demonstrate the effects of the new control inputs on the MMCs state variable errors and its dynamic. In addition, the carrier phase shifted modulation strategy is used because of applying the few number of converter modules to the MVDC system for ships. Moreover, relying on the proposed control strategy, a simulation model is built in MATLAB/SIMULINK software, where simulation results are utilized to verify the validity of proposed control strategy in the MMC-based MVDC system for ships.

key words: modular multilevel converter, MVDC, Lyapunov theory, circulating current, carrier phase shifted modulation

1. Introduction

Research trends worldwide have started to reconsider direct current (DC) power for future transmission and distribution system applications on ships. In the 21st century, the power system is going to DC while the power electronics technology progress, efficient of semiconductors and devices [1]. Nevertheless, medium voltage direct current power systems applied to all-electric ships pose several technical challenges [2]–[4], like system protection [5] and network stability [6], [7], accompanied by the large medium voltage loads on all-electric ships, for example pulse loads, propulsion drives and dedicated high power loads, medium voltage DC power system is gradually applied to all-electric ships [8]. Distinguished features of modular multilevel converters, including excellent quality output waveforms, transformerless performance, easy redundancy of sub-modules (SMs), desired output voltages and currents with easy redundancy, easy scalability and also simple fault detection and clearance promoted the utilization of MMCs in medium voltage applications [9]–[14].

Due to the importance of MMCs stable performance, the control and operation analysis of MMCs utilized in MVDC applications on ships has become a priority for researchers to attain a stable operating condition [15], [16]. For this reason, ref [17], [18] has been presented the challenges regarding the control system design for MMCs. In [19] a coordinated control based on direct Lyapunov theory is designed to assess the global asymptotical stability of a multi-terminal MMC-based HVDC system during varying both loads and DC link voltage. The desired DC-link voltage, active and reactive power variation have been the key factors for analyzing detailed mathematical models of MMCs utilized in HVDC applications in [20]. Reference [18] has been presented a control technique based on detailed mathematical models of MMCs to deal with robustness for MMC against varied load and parameters conditions. A sliding mode variable structure control strategy based on feedback linearization has been proposed to provide good robustness against system parameter deviations in [21]. On the other hand, another issue that is a reduced-order model for the MMC should be considered, the aim was to deal with electromechanical-transient simulations and small-signal analysis [22], including the inner control loops, the outer control loops and the strategy to balance the floating capacitor voltages [23]. And the inner control loops with high response dynamic using the exact discrete-time models plays an important role for controllers designed [24].

Considering MVDC power systems of all-electric ships requiring a control system that can ensure voltage stability and power flow control [7], circulating current suppression has been other matter for stability of the MMC because there is unbalanced distribution voltage between sub-modules when MMC is running normally [25]. In order to suppress the circulating current that improved small-signal stability with circulating current suppression controller [26], ref [27] has presented an improved proportional resonance (IPR) control circulating current suppression method. A novel fuzzy controller-based technique that maintains the natural balancing property of DC bus system is used to control the harmonics of the circulating currents in pulse width modulation (PWM) based MMCs [28]. In contrast, a digital plug-in repetitive controller that designed to control a carrier-phase-shift pulse-width-modulation (CPSM-PWM)-based MMC has the better performance of circulating harmonic current suppression [29]. Moreover, Ref. [30] has been proposed a strategy that use the compensation of DC-

Manuscript received October 11, 2021.

Manuscript revised January 29, 2022.

Manuscript publicized May 9, 2022.

[†]The authors are with Shanghai Maritime University, Pu-dong, Shanghai 201306, China.

^{††}The author is with Gdynia Maritime University, Gdynia 70213, Poland.

a) E-mail: liang_fang1997@163.com

DOI: 10.1587/transele.2021ESP0002

link voltage to suppress low-order circulating currents.

Because of the nonlinearity features of dynamic models of MMC-based MVDC system, many nonlinear strategies [31]–[33] can be presented for accurate control of such system. In [34], the global asymptotical stability of the MMC in HVDC system application has been considered by using the direct Lyapunov method. In addition, [35] has presented a control strategy based on the input-output feedback linearization theory combined with Lyapunov method to regulate the performance of MMC-based HVDC system under load variation and fault condition.

In this paper, a coordinated Lyapunov-based control technique is presented for the MMC-based MVDC system on ships using a new set of dynamic equations. The proposed controller aims at providing stable frequency and voltage magnitude of AC marine electric network in presence of both load variation and DC-link voltage fluctuations. The main contributions are illustrated as follows:

1) Obtaining a comprehensive dynamic mathematical model for based MMC-based MVDC system with four independent dynamical state variables, including AC-part currents and MMC-part circulating currents.

2) By the use of feedback linearization theory applied to the dynamic mathematical model, the new control inputs variables can be obtained.

3) Based on the new control inputs variables obtained, the Lyapunov function was designed to get some effective compensators for all control inputs of MMC for global asymptotical stable behavior of MMCs in MVDC system application.

2. The Mathematical Model of MMC- MVDC System

This paper investigates the MMC-based MVDC system on ships shown in Fig. 1 (a). According to this figure, the MMC along with both resistance and inductance to respectively mimic arm losses and limit arm-current harmonics and fault currents in each arm and its output is connected to an AC grid. Each MMC is composed of five SMs that are an IGBT half-bridge converter in its either upper or lower arms. A three-phase power supply provided by the ship diesel generators will be connected to the rectifier-mode MMC that provides a desire DC-link voltage. On the other side, it is assumed that active and reactive power AC loads can be fluctuated through the inverter-mode MMC provided by the DC-link voltage.

2.1 The Dynamic Model of MMC

In order to describe the proposed mathematical model of MMC-based MVDC system, a single-phase equivalent current diagram is depicted in Fig. 1 (b). By applying KVL's law from DC-link to output side of the MMC, the following dynamic mathematical models between input and output state variables are obtained.

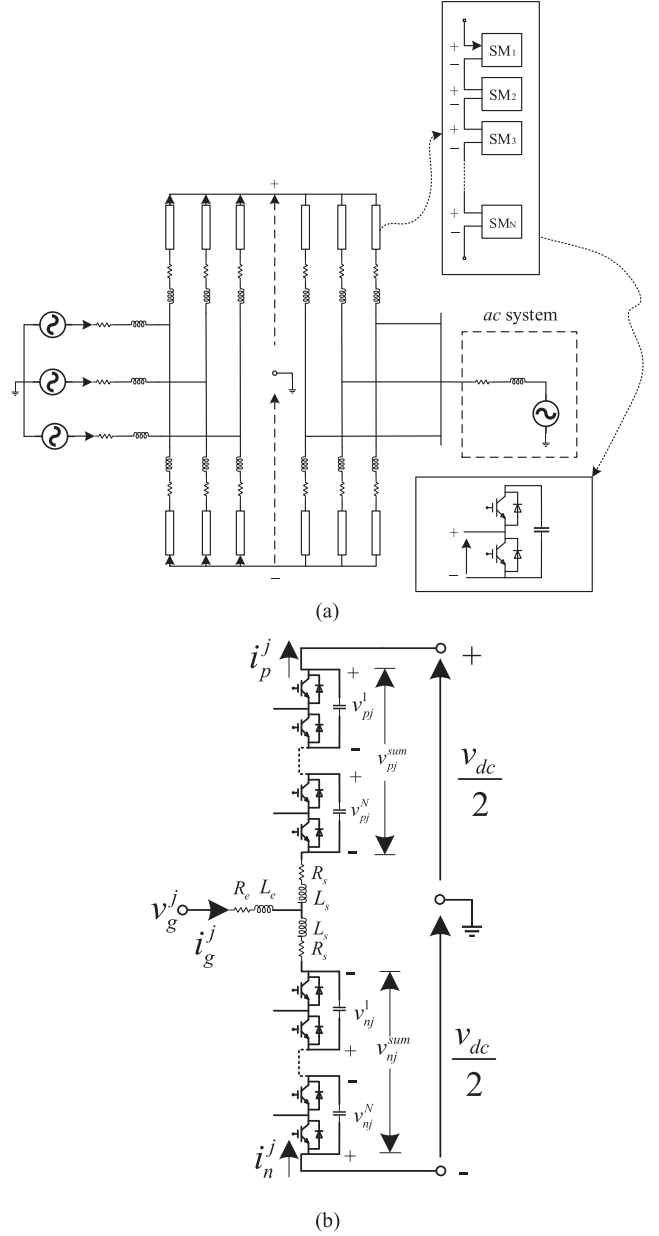


Fig. 1 The MMC-based MVDC studied on ships in this paper. (a) Detail of the converter arm. (b) A single-phase equivalent schematic diagram of the MMC.

$$\begin{aligned} v_g^j &= \frac{v_{dc}}{2} - v_{pj}^{sum} - R_s i_p^j - L_s \frac{di_p^j}{dt} - R_e i_g^j - L_e \frac{di_g^j}{dt} \\ v_g^j &= -\frac{v_{dc}}{2} + v_{nj}^{sum} + R_s i_n^j + L_s \frac{di_n^j}{dt} - R_e i_g^j - L_e \frac{di_g^j}{dt} \end{aligned} \quad (1)$$

Where R_s and L_s respectively is the MMC branch resistance and inductance, “ j ” demonstrates the abbreviation state-ments of three phases that are “ a ”, “ b ”, and “ c ” respectively. v_{pj}^{sum} and v_{nj}^{sum} is sum of upper and lower arms capacitor voltage, respectively.

Whereas applying KCL's law to the midpoint of the phase-leg gives:

$$i_g^j = i_p^j - i_n^j \quad (2)$$

Because of unequal voltages among the leg, the MMC has a current referred to as circulating current that can circulate within the three phases. And this circulating current is of double frequency negative sequence property. It is no effect on the external system including DC and AC for the circulating current. As shown in Fig. 1 (a), due to the symmetry of the three phase units, the DC side current i_{dc} (Actually, the direct current i_{dc} is equivalent to the ideal DC current I_{dc}) is evenly distributed among the three phase units, the DC component current in each phase unit is $\frac{i_{dc}}{3}$. The upper and lower arms currents can be defined as [36]:

$$\begin{aligned} i_p^j &= \frac{i_{dc}}{3} + \frac{i_g^j}{2} + i_{cir}^j \\ i_n^j &= \frac{i_{dc}}{3} - \frac{i_g^j}{2} + i_{cir}^j \end{aligned} \quad (3)$$

By summing up, the circulating current can be obtained,

$$i_{cir}^j = \frac{i_p^j + i_n^j}{2} - \frac{i_{dc}}{3} \quad (4)$$

The sum of the capacitor voltages of the upper and lower arms and the difference between the overall capacitor voltage of the upper and lower bridge arms is written as, respectively:

$$\begin{aligned} v_{sm}^{\sum j} &= v_{pj}^{\sum} + v_{nj}^{\sum} \\ v_{sm}^{\Delta j} &= v_{pj}^{\sum} - v_{nj}^{\sum} \end{aligned} \quad (5)$$

The relation (2), (4) and (5) is substituted into (1) leading to the dynamic mathematical Eqs. (6):

$$\begin{aligned} v_g^j + \frac{v_{sm}^{\Delta j}}{2} + R_z i_g^j + L_z \frac{di_g^j}{dt} &= 0 \\ v_{dc} - v_{sm}^{\sum j} - 2R_s i_{cir}^j - \frac{2}{3} R_s i_{dc} - 2L_s \frac{di_{cir}^j}{dt} &= 0 \end{aligned} \quad (6)$$

Where $R_z = \frac{R_s}{2} + R_e$, $L_z = \frac{L_s}{2} + L_e$.

The proposed dynamic mathematical equations can be achieved according to (6). Except for v_{dc} and v_g , it can be realized that the Eqs. (6) includes only upper and lower state variable, and circulating current respectively. These variables will promote more effective components for steady-state and dynamic parts of proposed control strategy. By applying the Park's transformation (7) to the AC side current equation of (6), where the angular frequency is fundamental frequency, and by applying the Park's transformation (7) to the circulating current equation of (6), where the angular frequency is double frequency and the phase sequence of the Park's transformation is a - c - b , the dynamic mathematical equations of the MVDC system in d-q can be presented in Eq. (8) as:

$$T_{abc/dq} = \frac{2}{3} \begin{bmatrix} \cos \theta & \cos(\theta - \frac{2}{3}\pi) & \cos(\theta + \frac{2}{3}\pi) \\ -\sin \theta & -\sin(\theta - \frac{2}{3}\pi) & -\sin(\theta + \frac{2}{3}\pi) \end{bmatrix} \quad (7)$$

$$\begin{aligned} v_g^d + \frac{v_{sm}^{\Delta d}}{2} + R_z i_g^d + L_z \frac{di_g^d}{dt} - \omega L_z i_g^q &= 0 \\ v_g^q + \frac{v_{sm}^{\Delta q}}{2} + R_z i_g^q + L_z \frac{di_g^q}{dt} + \omega L_z i_g^d &= 0 \\ v_{sm}^{\sum d} + 2R_s i_{cir}^d + 2L_s \frac{di_{cir}^d}{dt} - 4\omega L_s i_{cir}^q &= 0 \\ v_{sm}^{\sum q} + 2R_s i_{cir}^q + 2L_s \frac{di_{cir}^q}{dt} + 4\omega L_s i_{cir}^d &= 0 \end{aligned} \quad (8)$$

According to (8), The MMC AC side current and the circulating current d-q equations of the upper and lower arms can be written as the state equation:

$$\begin{aligned} \frac{d}{dt} \begin{bmatrix} i_g^d \\ i_g^q \\ i_{cir}^d \\ i_{cir}^q \end{bmatrix} &= \begin{bmatrix} -\frac{v_g^d}{L_z} - \frac{R_z}{L_z} i_g^d + \omega i_g^q \\ -\frac{v_g^q}{L_z} - \frac{R_z}{L_z} i_g^q - \omega i_g^d \\ -\frac{R_s}{L_s} i_{cir}^d + 2\omega i_{cir}^q \\ -\frac{R_s}{L_s} i_{cir}^q - 2\omega i_{cir}^d \end{bmatrix} \\ &+ \begin{bmatrix} -\frac{1}{2L_z} & 0 & 0 & 0 \\ 0 & -\frac{1}{2L_z} & 0 & 0 \\ 0 & 0 & -\frac{1}{2L_s} & 0 \\ 0 & 0 & 0 & -\frac{1}{2L_s} \end{bmatrix} \begin{bmatrix} v_{sm}^{\Delta d} \\ v_{sm}^{\Delta q} \\ v_{sm}^{\sum d} \\ v_{sm}^{\sum q} \end{bmatrix} \end{aligned} \quad (9)$$

2.2 Feedback Linearization

Feedback linearization is a powerful method for linearization and decoupling control of affine nonlinear systems. In this paper, feedback linearization theory is used for controller design. In general, input-output system can be defined as:

$$\begin{aligned} \dot{x} &= f(x) + g(x)u \\ y &= h(x) \end{aligned} \quad (10)$$

Where $f: D \rightarrow R^n$ and $g: D \rightarrow R^n$.

The derivative with the output y is calculated as follows:

$$y^{(\rho)} = L_f^\rho h(x) + L_g L_f^{\rho-1} h(x)u \quad (11)$$

In (11), if $L_g L_f^{i-1} h(x) \neq 0$ $i = 1, 2, \dots, \rho - 1$, the control input of the system can be written as,

$$u = \frac{1}{L_g L_f^{\rho-1} h(x)} [-L_f^\rho h(x) + v] \quad (12)$$

Equation (9) can be written the general form of the MVDC system by the help of (12) as follows:

$$u = \begin{bmatrix} v_{sm}^{\Delta d} \\ v_{sm}^{\Delta q} \\ v_{sm}^{\Sigma d} \\ v_{sm}^{\Sigma q} \end{bmatrix} = -2 \begin{bmatrix} L_z \dot{y}_1 \\ L_z \dot{y}_2 \\ L_s \dot{y}_3 \\ L_s \dot{y}_4 \end{bmatrix} + 2 \begin{bmatrix} -v_g^d - R_z i_g^d + \omega L_z i_g^q \\ -v_g^q - R_z i_g^q - \omega L_z i_g^d \\ -R_s i_{cir}^d + 2\omega L_s i_{cir}^q \\ -R_s i_{cir}^q - 2\omega L_s i_{cir}^d \end{bmatrix} \quad (13)$$

Where the output of proposed control strategy can be presented as:

$$y = [y_1 \quad y_2 \quad y_3 \quad y_4]^T = [i_g^d \quad i_g^q \quad i_{cir}^d \quad i_{cir}^q]^T \quad (14)$$

3. Proposed Control Strategy

3.1 Proposed Compensators Based on Lyapunov Theory

In order to investigate the stability of the MVDC system on ships through varying the proposed control inputs in (14), an energy function should be defined to satisfy conditions given in (15),

$$\begin{aligned} V(x) &\rightarrow \infty \quad \text{as } \|x\| \rightarrow \infty \\ \dot{V}(x) &< 0 \quad \forall x \neq 0 \end{aligned} \quad (15)$$

To this end, the following Lyapunov energy function will be defined for the MMC-based MVDC system,

$$\begin{aligned} V = & \frac{1}{4} \lambda_1 \|v_{sm}^{\Delta d} - v_{sm}^{\Delta d*}\|^2 + \frac{1}{4} \lambda_2 \|v_{sm}^{\Delta q} - v_{sm}^{\Delta q*}\|^2 \\ & + \frac{1}{4} \lambda_3 \|v_{sm}^{\Sigma d} - v_{sm}^{\Sigma d*}\|^2 + \frac{1}{4} \lambda_4 \|v_{sm}^{\Sigma q} - v_{sm}^{\Sigma q*}\|^2 \end{aligned} \quad (16)$$

Where $\lambda_1 \sim \lambda_4$ is the energy factors of function, respectively.

In fact, it is guaranteed that the error dynamics of MMCs can lead to asymptotical global stability for the MMC-based MVDC system by using the Lyapunov method. The derivative of (17) should be obtained,

$$\begin{aligned} \dot{V} = & \frac{1}{2} \lambda_1 (v_{sm}^{\Delta d} - v_{sm}^{\Delta d*}) (\dot{v}_{sm}^{\Delta d} - \dot{v}_{sm}^{\Delta d*}) \\ & + \frac{1}{2} \lambda_2 (v_{sm}^{\Delta q} - v_{sm}^{\Delta q*}) (\dot{v}_{sm}^{\Delta q} - \dot{v}_{sm}^{\Delta q*}) \\ & + \frac{1}{2} \lambda_3 (v_{sm}^{\Sigma d} - v_{sm}^{\Sigma d*}) (\dot{v}_{sm}^{\Sigma d} - \dot{v}_{sm}^{\Sigma d*}) \\ & + \frac{1}{2} \lambda_4 (v_{sm}^{\Sigma q} - v_{sm}^{\Sigma q*}) (\dot{v}_{sm}^{\Sigma q} - \dot{v}_{sm}^{\Sigma q*}) \end{aligned} \quad (17)$$

Considering the complexity of the formula, it is assumed that $e_g^d = i_g^d - i_g^{d*}$, $e_g^q = i_g^q - i_g^{q*}$, $e_{cir}^d = i_{cir}^d - i_{cir}^{d*}$, $e_{cir}^q = i_{cir}^q - i_{cir}^{q*}$, $\lambda_{cir} = \lambda_3 = \lambda_4$, $\dot{v}_g^d - \dot{v}_g^{d*} = \dot{v}_g^q - \dot{v}_g^{q*} = 0$, $\lambda_g = \lambda_1 = \lambda_2$, $\dot{i}_g^q - \dot{i}_g^{q*} = \dot{i}_g^d - \dot{i}_g^{d*} = \dot{i}_{cir}^q - \dot{i}_{cir}^{q*} = \dot{i}_{cir}^d - \dot{i}_{cir}^{d*} = 0$.

Therefore, the formula can simplify to (18),

$$\begin{aligned} \dot{V} = & \lambda_g (L_z R_z \dot{e}_g^d + R_z (v_g^d - v_g^{d*}) + \omega L_z (v_g^q - v_g^{q*}) \\ & + \omega^2 L_z^2 e_g^d + R_z^2 e_g^d) \dot{e}_g^d \\ & + \lambda_g (L_z R_z \dot{e}_g^q + R_z (v_g^q - v_g^{q*}) - \omega L_z (v_g^d - v_g^{d*}) \\ & + (\omega^2 L_z^2 + R_z^2) e_g^q) \dot{e}_g^q \\ & + \lambda_{cir} (L_s R_s \dot{e}_{cir}^d + (4\omega^2 L_s^2 + R_s^2) e_{cir}^d) \dot{e}_{cir}^d \\ & + \lambda_{cir} (L_s R_s \dot{e}_{cir}^q + (4\omega^2 L_s^2 + R_s^2) e_{cir}^q) \dot{e}_{cir}^q \end{aligned} \quad (18)$$

In order to reach a global stable MMC-based MVDC system, the derivative of Lyapunov function in (18) must be negative. If $\dot{V} < 0$, each sub-part of the function (18) must be negative, respectively. It is assumed as the follows:

$$\begin{aligned} \alpha_g^d \lambda_g \dot{e}_g^d &= L_z R_z \dot{e}_g^d + R_z (v_g^d - v_g^{d*}) \\ & + \omega L_z (v_g^q - v_g^{q*}) + (\omega^2 L_z^2 + R_z^2) e_g^d \\ \alpha_g^q \lambda_g \dot{e}_g^q &= L_z R_z \dot{e}_g^q + R_z (v_g^q - v_g^{q*}) \\ & - \omega L_z (v_g^d - v_g^{d*}) + (\omega^2 L_z^2 + R_z^2) e_g^q \\ \alpha_{cir}^d \lambda_{cir} \dot{e}_{cir}^d &= L_s R_s \dot{e}_{cir}^d + (4\omega^2 L_s^2 + R_s^2) e_{cir}^d \\ \alpha_{cir}^q \lambda_{cir} \dot{e}_{cir}^q &= L_s R_s \dot{e}_{cir}^q + (4\omega^2 L_s^2 + R_s^2) e_{cir}^q \end{aligned} \quad (19)$$

The relation (19) will be substituted into (18) leading to the Eq. (20),

$$\begin{aligned} \dot{V} = & \alpha_g^d \lambda_g^2 (\dot{e}_g^d)^2 + \alpha_g^q \lambda_g^2 (\dot{e}_g^q)^2 \\ & + \alpha_{cir}^d \lambda_{cir}^2 (\dot{e}_{cir}^d)^2 + \alpha_{cir}^q \lambda_{cir}^2 (\dot{e}_{cir}^q)^2 \end{aligned} \quad (20)$$

Where α_g^d , α_g^q , α_{cir}^d and α_{cir}^q are Lyapunov coefficients that should be negative. By rearranging the terms in (19), the dynamic compensation parts of proposed modulation functions can be meet,

$$\begin{aligned} e_g^d &= [R_z (v_g^d - v_g^{d*}) + \omega L_z (v_g^q - v_g^{q*})] f_g^d \\ e_g^q &= [R_z (v_g^q - v_g^{q*}) - \omega L_z (v_g^d - v_g^{d*})] f_g^q \\ e_{cir}^d / f_{cir}^d &= 0 \\ e_{cir}^q / f_{cir}^q &= 0 \end{aligned} \quad (21)$$

Where

$$\begin{aligned} f_g^d &= \frac{1}{(\alpha_g^d \lambda_g - L_z R_z) s - (\omega^2 L_z^2 + R_z^2)} \\ f_g^q &= \frac{1}{(\alpha_g^q \lambda_g - L_z R_z) s - (\omega^2 L_z^2 + R_z^2)} \\ f_{cir}^d &= \frac{1}{(\alpha_{cir}^d \lambda_{cir} - L_s R_s) s - (4\omega^2 L_s^2 + R_s^2)} \\ f_{cir}^q &= \frac{1}{(\alpha_{cir}^q \lambda_{cir} - L_s R_s) s - (4\omega^2 L_s^2 + R_s^2)} \end{aligned} \quad (22)$$

For the circulating current control, the circulating current in the formula (21) can be rewritten as follows:

$$e_{cir}^d / f_{cir}^d = e_{cir}^q / f_{cir}^q = 0 \quad (23)$$

So, the dynamic circulating current compensation parts of proposed modulation functions can be meet,

$$\begin{aligned} e_{cir}^d \cdot f_{cir}^q &= 0 \\ e_{cir}^q \cdot f_{cir}^d &= 0 \end{aligned} \quad (24)$$

The detailed schematic of proposed control technique is illustrated in Fig. 2 by formula (8) and (21) and (24). According to this figure, MMC output and circulating currents are both involved with the proposed compensators. For the AC

side current control, the f_g^d is a transfer function. e_g^d is determined jointly by f_g^d and its molecule. Similarly, the f_g^q is a transfer function. The purpose is to execute more accurate tracking of the state variables errors fluctuations. For the circulating current control, there is a cross connection in d-q in Fig. 2 because of formula (24).

3.2 CPSM—Based Voltage Balancing Method

Carrier phase shift modulation (CPSM) that is another MMC modulation strategy that is different from NLM, is a kind of pulse width modulation. Schematic diagram of half-bridge MMC carrier phase-shift modulation is illustrated in Fig. 3. According to the figure, each bridge arm has N carriers, the phase difference between adjacent carriers is $2\pi/N$, and the phase angle is θ between the upper and lower bridge arms that have a reference voltage $v_{\text{ref-pj}}$ and $v_{\text{ref-nj}}$.

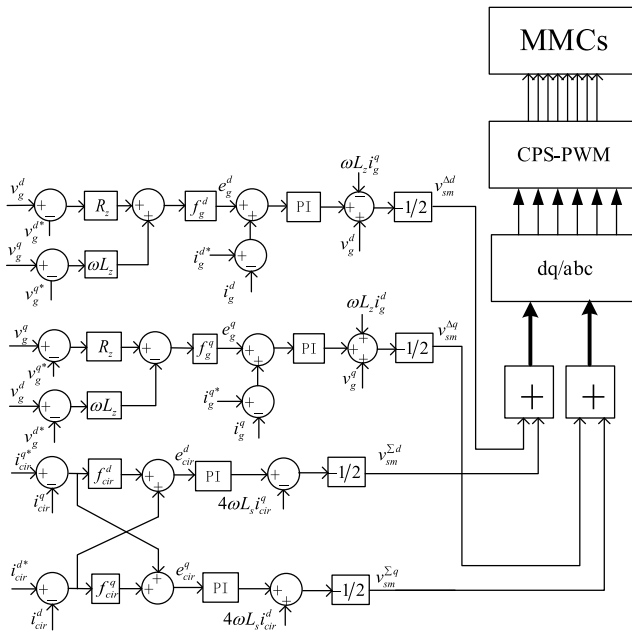


Fig. 2 Overall structure of the proposed control strategy.

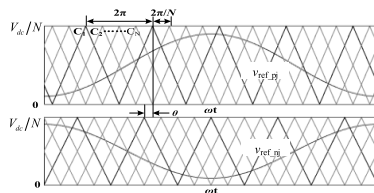


Fig. 3 Schematic diagram of half-bridge MMC carrier phase-shift modulation.

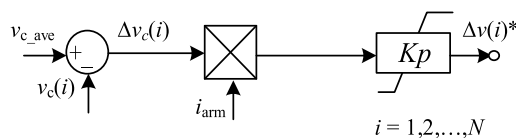


Fig. 4 An additional balance control strategy.

In order to avoid the demand to the internal voltage of the bridge arm and the voltage of the upper and lower bridge arms in the traditional method, an additional balance control strategy shown in Fig. 4 is proposed by directly using the instantaneous average value of the bridge arm voltage as a reference.

Figure 4 shows that the reference voltage for the upper and lower arms of the j^{th} phase after adding the balance control can be obtained,

$$\begin{aligned} v_{\text{ref-nj}}(i) &= \frac{V_{\text{dc}}}{2N} \left(1 + M \cos(\omega_0 t + \phi_j) \right) + \Delta v_{\text{nj}}(i) \\ v_{\text{ref-pj}}(i) &= \frac{V_{\text{dc}}}{2N} \left(1 + M \cos(\omega_0 t + \phi_j + \pi) \right) + \Delta v_{\text{pj}}(i) \end{aligned} \quad (25)$$

Where $v_{c,\text{ave}}$ is the instantaneous average value of the voltage of N sub-modules of the bridge arm, $v_c(i)$ and $\Delta v_c(i)$ is capacitor voltage of the i^{th} sub-module in the bridge arm and the difference between the capacitor voltage of the i^{th} module and the instantaneous average voltage, respectively, i_{arm} is current of the bridge arm of sub-module. And $\Delta v(i)^*$ is compensation voltage.

4. Simulation Results and Discussion

The MMC-based MVDC system on ships is simulated in MTALAB/SIMULINK soft-ware, when the proposed control strategy is applied as depicted in Fig. 2. The parameters of the considered MMC-based MVDC system on ships are given in Table 1.

To show effectively the impact of proposed control strategy on the stability of the MMC-based MVDC system, two simulation process will be considered. In the first situation, the load on the electricity unit on the ship is altered to test the performance of the proposed control strategy. In the second situation, the conventional controller is used in the first process, while the proposed control method is employed in the second process. The results are presented and discussed in the following section.

4.1 DC-Link and the Inverter-Side MMC under Multi-Style Loading Conditions

In order to check the dynamic performance of the MMC-based MVDC system, firstly, a load of 3 MW connected to

Table 1 Simulation parameters.

Description	Value
Rectifier-side MMC SM capacitor	3 mF
Rectifier-side MMC arm inductance	2.5 mH
Rectifier-side MMC arm resistance	0.2 Ω
inverter-side MMC arm inductance	2 mF
inverter-side MMC arm resistance	8 mH
inverter-side MMC arm resistance	0.2 Ω
DC-link voltage	6 kV
f_s (Switching Frequency)	0.8 kHz
f_{ac} (AC Voltage Frequency)	50 Hz
AC phase voltage rating	3.5 kV

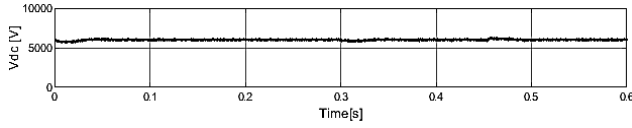


Fig. 5 The DC-link voltage of the considered MMC-based MVDC system during load variation.

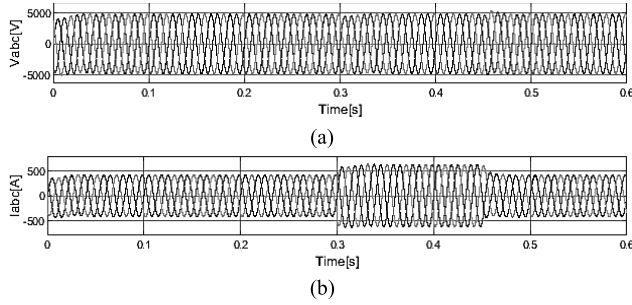


Fig. 6 The AC-part output voltage and current during load variation. (a) The AC-part output voltage. (b) The AC-part output current.

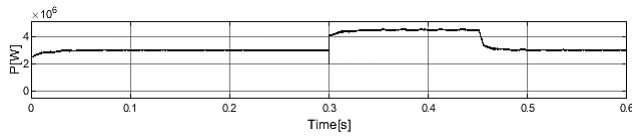


Fig. 7 The AC-part active power during load variation.

the output of the AC-part is supplied by the MVDC system. Secondly, the power consumption is increased by another load of 1.5 MW at $t = 0.3$ s. Lastly, at $t = 0.45$ s, the load of 1.5 MW will be disconnected from the output of the AC-part of MVDC system.

The DC-link voltage of the considered MMC-based MVDC system during the load step variation is illustrated in Fig. 5. According to the figure, the DC-link voltage is fluctuated with both steady-state and dynamic errors and can be kept as its desired value 6 kV when the power consumption is increased at $t = 0.3$ and the power consumption is decreased at $t = 0.45$ s.

Figure 6 shows the AC-part output voltage and current during the load step variation. It can be seen from the figure that the output voltage and current waveforms have a good sinusoidal wave with very low THD. When the load of AC-part of MVDC system is increased at $t = 0.3$ s and decreased at $t = 0.45$ s, the output voltage and current both can follow up their desired values with a small transient time as shown in Fig. 6.

The AC-part active power during the load step variation is presented in Fig. 7. As it can be understood from this figure that the MMCs can be to track their reference values under the load variations. During the load variations, the MMCs can appropriately increase or decrease the needed active power with negligible fluctuations and fast dynamic response.

Figure 8 illustrates the inverter-part MMCs SM capacitor voltage during the load step variation. It is obvious from

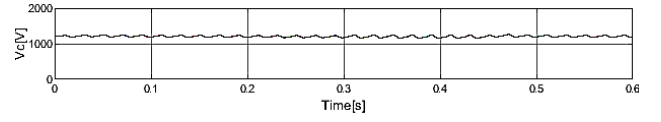


Fig. 8 The inverter-part MMCs SM capacitor voltage during load variation.

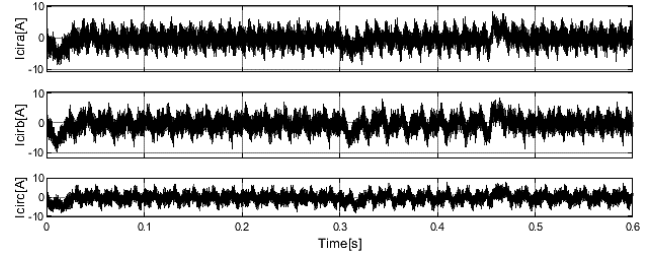


Fig. 9 The inverter-part MMCs circulating currents during load variation.

this figure that the SM capacitor voltage of the MMCs can be kept balance with maximum voltage deviation of 80 V. The voltage deviation is an acceptable value for the MVDC system in both steady state and dynamic conditions.

The inverter-part MMCs circulating currents during the load step variation is shown in Fig. 9. From circulating current waveforms of Fig. 9, it can be derived that these currents in MMCs are properly reduced by the steady state section of the proposed control strategy especially in comparison with the magnitude of output currents presented in Fig. 6 (b) during sudden loads variation.

According to the analysis in Fig. 5-9, there is no considerable dynamic to be seen in the state variable responses of the dc-part and AC-part during sudden loads variation. Based on the above analysis, it can be verified the dynamic performance of the proposed control strategy to apply the MMC-based MVDC system on ships.

4.2 Comparison and Analysis MMCs under Multi-Style Loading Conditions

To show effectively the impact of the proposed control strategy, two simulation processes will be considered. The one is simulation processes without proposed control strategy, the other one is simulation processes with proposed control strategy. And at the beginning, a load of 3 MW connected to the output of the AC-part is supplied. At $t = 0.3$ s, the power consumption is increased by another load of 1.5 MW.

Figure 10 shows the DC-link voltage of the MMC-based MVDC system, where Fig. 10 (a) is the DC-link voltage without proposed control strategy and Fig. 10 (b) is the DC-link voltage with proposed control strategy. It is obvious from the two figures that the DC-link voltage by applying proposed control strategy with steady-state and dynamic errors during the entire simulation time is better than the DC-link voltage without proposed control strategy. Especially at $t = 0.3$ s, the DC-link voltage without proposed control strategy has dropped significantly.

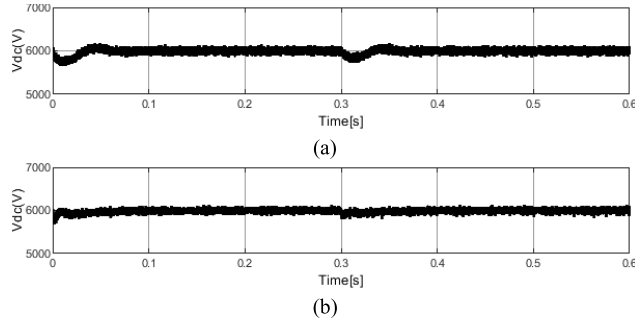


Fig. 10 The DC-link voltage of the MMC-based MVDC system. (a) The DC-link voltage without proposed control strategy. (b) The DC-link voltage with proposed control strategy.

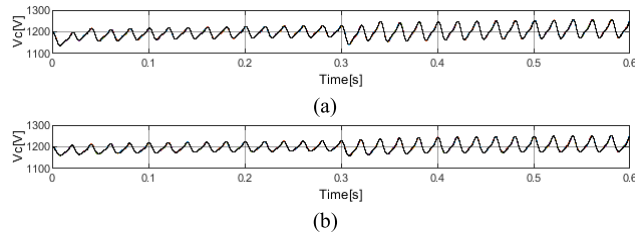


Fig. 11 The inverter-part MMCs SM capacitor voltage of the MMC-based MVDC system. (a) The inverter-part MMCs SM capacitor voltage without proposed control strategy. (b) The inverter-part MMCs SM capacitor voltage with proposed control strategy.

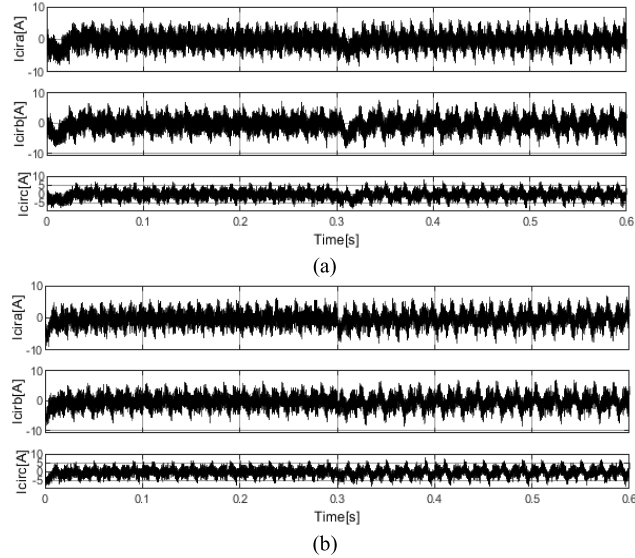


Fig. 12 The inverter-part MMCs circulating currents of the MMC-based MVDC system. (a) The inverter-part MMCs circulating currents without proposed control strategy. (b) The inverter-part MMCs circulating currents with proposed control strategy.

The inverter-part MMCs SM capacitor voltage of the MMC-based MVDC system is illustrated in Fig. 11. The inverter-part MMCs SM capacitor voltage has higher quality waveform during both dynamic and steady operation of the proposed control strategy. When the power consumption is increased by another load at $t = 0.3s$, the SM capacitor

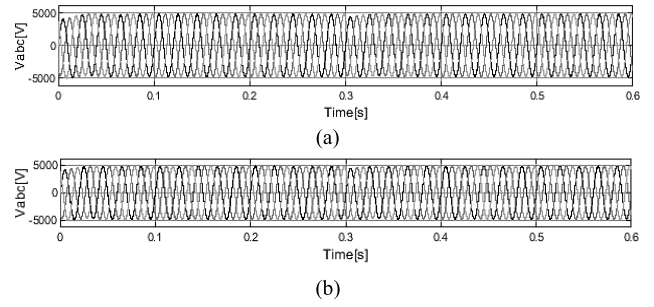


Fig. 13 The AC-part output voltage of the MMC-based MVDC system. (a) The AC-part output voltage without proposed control strategy. (b) The AC-part output voltage with conventional control strategy.

voltage with the conventional control strategy is noticeably increased, while the SM capacitor voltage with the proposed control strategy has little voltage change. Figure 12 shows the inverter-part MMCs circulating currents of the MMC-based MVDC system. According to the two figures, the inverter-part MMCs circulating currents amplitude with proposed control strategy is a little smaller than circulating currents values with the conventional control strategy.

Figure 13 illustrates the AC-part output voltage of the MMC-based MVDC system with the conventional control strategy and the proposed control strategy. When the power consumption is increased by another load at $t = 0.3s$, the voltage amplitude with the conventional control strategy drops more than the voltage amplitude with the proposed control strategy. From the Fig. 10-13, it can be verified the superiority of proposed control technique.

5. Conclusion

The stable operating conditions of the MMC-based MVDC transmission system for ships have been proposed in this paper through the use of feedback linearization theory applied to the dynamic equations with Lyapunov theory-based first-order compensators. Firstly, a set of dynamics equations is proposed based on separating the dynamics of AC-part currents and MMCs circulating currents. These state variables have been set to make dynamic mathematic functions with MMC's circulating currents and output currents in d-q reference frame. Based on the dynamic mathematic functions of MMC, the new control inputs can be obtained by the use of feedback linearization theory applied to the dynamic functions. Moreover, based on the new control inputs variables obtained, the Lyapunov function was designed to get some effective compensators for all control inputs of MMCs. Also, it has been contributed to demonstrate the effects of the new control inputs on the MMCs state variable errors and its dynamic. In addition, considering the usage restrictions of number of the sub-modules on ships, the carrier phase shifted modulation strategy is applied to the MMC-based MVDC system. Lastly, by using MATLAB/SIMULINK software, it has been verified accurate steady state and dynamic responses of proposed control strategy under variation of load and Controllers used or not.

Although the results have been verified by simulation, experiments can be used to verify the proposed control strategy in the future work to find more problems to solve.

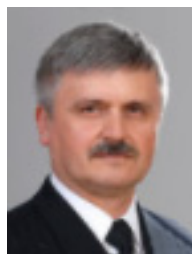
Acknowledgments

This research was funded by 2021-2022 China-Poland S&T Cooperation Project (No.19), Shanghai S&T Commission under Grant 1904050170 & 20040501200.

References

- [1] Q. Sun, Y. Wang, G. Liu, J. Meng, Q. Mu, X. Zhang, and Y. Li, "A high-frequency-link voltage matching phase-shift control strategy for high-frequency modular multilevel DC transformer in MVDC distribution networks," *Electr. Power Syst. Res.*, vol.175, pp.1–10, 2019. DOI: 10.1016/j.epsr.2019.105922
- [2] R.D. Geertsma, R.R. Negenborn, K. Visser, and J.J. Hopman, "Design and control of hybrid power and propulsion systems for smart ships: A review of developments," *Appl. Energy*, vol.194, pp.30–54, 2017. DOI: 10.1016/j.apenergy.2017.02.060
- [3] N. Doerry, "Naval power systems-integrated power systems for the continuity of the electrical power supply," *IEEE Electrification Mag.*, vol.3, no.2, pp.12–21, 2015. DOI: 10.1109/MELE.2015.2413434
- [4] G. Sulligoi, A. Vicenzutti, and R. Menis, "All-electric ship design: from electrical propulsion to integrated electrical and electronic power systems," *IEEE Trans. Transp. Electrification*, vol.2, no.4, pp.507–521, 2016. DOI: 10.1109/TTE.2016.2598078
- [5] P. Cairoli and R.A. Dougal, "New horizons in DC shipboard power systems-new fault protection strategies are essential to the adoption of DC power systems," *IEEE Electrification Mag.*, vol.1, no.2, pp.8–45, 2013. DOI: 10.1109/MELE.2013.2291431
- [6] U. Javaid, F.D. Frejedo, D. Dujic, and W.V.D. Merwe, "Dynamic assessment of source-load interactions in marine MVDC distribution," *IEEE Trans. Ind. Electron.*, vol.64, no.6, pp.4372–4381, 2017. DOI: 10.1109/TIE.2017.2674597
- [7] M. Cupelli, F. Ponci, G. Sulligoi, A. Vicenzutti, C.S. Edrington, T. El-Mezyani, and A. Monti, "Power flow control and network stability in an all-electric ship," *Proc. IEEE*, vol.103, no.12, pp.2355–2380, 2015. DOI: 10.1109/JPROC.2015.2496789
- [8] S. Castellan, R. Menis, A. Tessarolo, F. Luise, and T. Mazzuca, "A review of power electronics equipment for all-electric ship MVDC power systems," *Int. J. Electr. Power Energy Syst.*, vol.96, pp.306–323, 2018. DOI: 10.1016/j.ijepes.2017.09.040
- [9] K. Shinoda, A. Benchaib, J. Dai, and X. Guillaud, "Virtual capacitor control: mitigation of DC voltage fluctuations in MMC-based HVdc systems," *IEEE Trans. Power Deliv.*, vol.33, no.1, pp.455–465, 2018. DOI: 10.1109/TPWRD.2017.2723939
- [10] J. Qin, M. Saeedifard, A. Rockhill, and R. Zhou, "Hybrid design of modular multilevel converters for HVDC systems based on various submodule circuits," *IEEE Trans. Power Deliv.*, vol.30, no.1, pp.385–394, 2015. DOI: 10.1109/TPWRD.2014.2351794
- [11] S.-M. Kim, M.-G. Jeong, J. Kim, and K.-B. Lee, "Hybrid modulation scheme for switching loss reduction in a modular multilevel high-voltage direct current converter," *IEEE Trans. Power Deliv.*, vol.34, no.4, pp.3178–3191, 2019. DOI: 10.1109/TPEL.2018.2848620
- [12] S. Li, Y. Xu, Y. Lu, C. Zhao, J. Zhang, C. Jiang, and S. Qiu, "An auxiliary DC circuit breaker utilizing an augmented MMC," *IEEE Trans. Power Deliv.*, vol.34, no.2, pp.561–571, 2019. DOI: 10.1109/TPWRD.2019.2892445
- [13] M. Mehra, R. Godina, E. Pouresmaeil, E.M.G. Rodrigues, and J.P.S. Catalão, "Power quality improvement with a pulse width modulation control method in modular multilevel converters under varying nonlinear loads," *Appl. Sci.*, vol.10, no.9, p.3292, May 2020. DOI: 10.3390/app10093292
- [14] L. Bessegato, L. Harnerfors, K. Ilves, and S. Norrga, "A method for the calculation of the AC-side admittance of a modular multilevel converter," *IEEE Trans. Power Deliv.*, vol.34, no.5, pp.4161–4172, 2019. DOI: 10.1109/TPEL.2018.2862254
- [15] M. Mehra: "Control of modular multilevel converters in high voltage direct current power system," Ph.D Dissertation, Universidade da Beira Interior, Portugal, 2019.
- [16] B. Li, H. Liu, W. Wen, H. Cao, X. Wang, and H. Lv, "DC faults ride-through and fast recovery of MVDC system based on improved HB-MMC," *IEEE J. Emerg. Sel. Topics Power Electron.*, vol.8, no.3, pp.3056–3066, June 2020. DOI: 10.1109/JESTPE.2019.2920372
- [17] M. Mehra, E. Pouresmaeil, S. Taheri, I. Vechiu, and J.P.S. Catalão, "Novel control strategy for modular multilevel converters based on differential flatness theory," *IEEE J. Emerg. Sel. Topics Power Electron.*, vol.6, no.2, pp.888–897, June 2018. DOI: 10.1109/jestpe.2017.2766047
- [18] M. Mehra, E. Pouresmaeil, M.F. Akorede, S. Zabihi, and J.P.S. Catalão, "Function-based modulation control for modular multilevel converters under varying loading and parameters conditions," *IET Gener. Transm. Dis.*, vol.11, no.13, pp.3222–3230, 2017. DOI: 10.1049/iet-gtd.2016.1028
- [19] R.J. Ghadia, M. Mehra, E.M. Adabi, and S. Bacha, "Lyapunov theory-based control strategy for multi-terminal MMC-HVDC systems," *Int. J. Electr. Power Energy Syst.*, vol.129, no.2, July 2021. DOI: 10.1016/j.ijepes.2021.106778
- [20] T. Stoetzel, M.K. Jger, C. Heising, and V. Staudt, "Analysis of DC-droop control for an MMC-Based HVDC system," *Mediterranean Conf. on Power Gener., Transm., Distrib. and Energy Conversion*, pp.1–7, Nov. 2016. DOI: 10.1049/cp.2016.1072
- [21] J.L. Yu, C.Y. Xia, and H.L. Miao, "Nonlinear control of modular multilevel converters," *Acta Energaie Solaris Sinica*, vol.41, no.5, pp.266–272, 2020.
- [22] H. Yang, Y. Dong, W. Li, and X. He, "Average-value model of modular multilevel converters considering capacitor voltage ripple," *IEEE Trans. Power Deliv.*, vol.32, no.2, pp.723–732, April 2017. DOI: 10.1109/TPWRD.2016.2555983
- [23] E.L. Andres and J.A. Santiago, "Modeling, control and reduced-order representation of modular multilevel converters," *IEEE Power Syst. Res.*, vol.163, pp.196–210, Oct. 2018. DOI: 10.1016/j.epsr.2018.05.024
- [24] A. Zama, A. Benchaib, S. Bacha, D. Frey, and S. Slivant, "High dynamics control for MMC based on exact discrete-time model with experimental validation," *IEEE Trans. Power Deliv.*, vol.33, no.1, pp.477–488, Feb. 2018. DOI: 10.1109/TPWRD.2017.2707343
- [25] X.T. Tan, H.M. Zhang, Y.Q. Zhu, and J.B. Chen, "Research on submodule capacitor voltage ripples and voltage balancing control strategy in modular multilevel converter," *Power Electron.*, vol.50, no.1, pp.1–4, 2016.
- [26] M. Zhang, Y. Shen, H. Sun, and R. Guo, "MMC-HVDC circulating current suppression method based on improved proportional resonance control," *Energy Rep.*, vol.6, no.9, pp.863–871, Dec. 2020. DOI: 10.1016/j.egy.2020.11.120
- [27] J. Freyte, G. Bergna, J.A. Suul, S. D'Arco, F. Gruson, F. Colas, H. Saas, and G. Xavier, "Improving small-signal stability of an MMC with CCSC by control of the internally stored energy," *IEEE Trans. Power Deliv.*, vol.33, no.1, pp.429–439, Feb. 2018. DOI: 10.1109/TPWRD.2017.2725579
- [28] T.S. Narayana and R. Dahiya, "DC-link voltage compensation with fuzzy-based MMC to mitigate the low-order circulating current," *Int. J. Ambient Energy*, vol.66, pp.1790–2022, 2021. DOI: 10.1080/01430750.2021.1876761
- [29] M. Zhang, L. Huang, W. Yao, and Z. Lu, "Circulating harmonic current elimination of a CPS-PWM based modular multilevel converter with plug-in repetitive controller," *IEEE Trans. Power Deliv.*, vol.29, no.4, pp.2083–2097, April 2014. DOI: 10.1109/TPEL.2013.

- 2269140
- [30] Y. Sun, C.A. Teixeira, D.G. Holmes, B.P. Mcgrath, and J. Zhao, "Low-order circulating current suppression of PWM-based modular multilevel converters using DC-link voltage compensation," *IEEE Trans. Power Deliv.*, vol.33, no.1, pp.210–225, Jan. 2018. DOI: 10.1109/TPEL.2017.2670369
 - [31] M. Mehrasa, M. Ahmadijorji, A. Abedi, and M.A. Reykandeh, "Dual lagrangian modeling and Lyapunov-based control three-level three-phase NPC voltage-source rectifier," *2012 11th Int. Conf. Environ. and Electr. Eng.*, pp.737–747, May 2012. DOI: 10.1109/EEEIC.2012.6221474
 - [32] M. Mehrasa, M. Ahmadijorji, and N. Amjadi, "A new dual lagrangian model and input/output feedback linearization control of 3-phase/level NPC voltage- source rectifier," *Automatika*, vol.55, no.1, pp.99–11, 2014. DOI: 10.7305/automatika.2014.01.230
 - [33] M. Ahmadijokani, M. Mehrasa, M. Sleiman, M. Sharifzadeh, A. Sheikholeslami, and K. Al-Haddad, "A back-stepping control method for modular multilevel converters," *IEEE Trans. Ind. Electron.*, vol.68, no.1, pp.443–453, Jan. 2021. DOI: 10.1109/TIE.2019.2962455
 - [34] M. Mehrasa, E. Pouresmaei, S. Zabihi, and J.P.S. Catalo, "Dynamic, model, control and stability analysis of MMC in HVDC transmission systems," *IEEE Manchester PowerTech.*, vol.32, no.3, pp.1471–1482, June 2017. DOI: 10.1109/PTC.2017.7981256
 - [35] N. Beheshti, M. Rezanejad, and M. Mehrasa, "Linearized control technique with Lyapunov function-based compensators for MMC-based HVDC system under load variation and fault condition," *Int. J. Electr. Power Energy Syst.*, vol.124, pp.1–15, Jan. 2021. DOI: 10.1016/j.ijepes.2020.106333
 - [36] J. Wang, R. Burgos, and D. Boroyevich, "Switching-cycle state-space modeling and control of the modular multilevel converter," *IEEE J. Emerg. Sel. Topics Power Electron.*, vol.2, no.4, pp.1159–1170, Nov. 2014. DOI: 10.1109/JESTPE.2014.2354393



He has been with the Gdynia Maritime University since 1994.

Tomasz Tarasiuk received the M.S. degree in marine electrical engineering from the Gdynia Maritime University in 1989, the Ph.D. degree in electrical engineering from the Gdańsk University of Technology in 2001, and the D.S. degree in electrical engineering (metrology and signal processing) from the Warsaw University of Technology in 2010. His research interest focuses on marine microgrids, particularly power quality and its assessment, including signal processing tools and methods.



Liang Fang received the B.S. and M.E. degrees in Electrical Engineering from Shanghai Maritime University in 2012 and 2018, respectively. The current main research direction is the stability of the ship's medium voltage DC bus. He is currently pursuing the Ph.D. degrees at Shanghai Maritime University.



Xiaoyan Xu received the B.S. and M.E. degrees in Electrical Engineering from Shanghai Maritime University in 1993 and 1996, respectively, the Ph.D. degree in power system automation from Gdansk University of Technology. He stayed in ship power parameter detection and power quality control. He now with Shanghai Maritime University. Currently teaching at Shanghai Maritime University.